Computers and Electronics in Agriculture 100 (2014) 131–138

Contents lists available at ScienceDirect

Computers and Electronics in Agriculture

journal homepage: www.elsevier.com/locate/compag

Vertical point sampling with a digital camera: Slope correction and field evaluation

Daniel S. Maynard [a,*], Mark J. Ducey [a], Russell G. Congalton [a], John Kershaw [b], Joel Hartter [c,1]

[a] University of New Hampshire, Department of Natural Resources & The Environment, 114 James Hall, 46 College Rd., Durham, NH 03824, USA
[b] University of New Brunswick, Faculty of Forestry & Environmental Management, P.O. Box 4400, 28 Dineen Drive, Fredericton, NB E3B 5A3, Canada
[c] University of New Hampshire, Department of Geography, 102 Huddleston Hall, 73 Main Street, Durham, NH 03824, USA

ARTICLE INFO

Article history:
Received 7 June 2013
Received in revised form 4 November 2013
Accepted 16 November 2013

Keywords:
Forest inventory
Probability proportional to size sampling
Point double sampling
Forest structure

ABSTRACT

Vertical point sampling with a digital camera (VPSC) is a promising new forest sampling method that can be used to improve existing sampling protocols or rapidly assess forest structure over large areas. Previous research into VPSC has not accounted for the potential bias that can result from implementing this method on sloping terrain. Here, we present a modified method of conducting VPSC on sloping terrain that maintains unbiased estimates by implementing an automated computer program to adjust for slope at each sample point. This updated method is easily implemented and includes minimal alterations to the existing VPSC protocol, though there will likely be some situations where it is impractical or unnecessary. To address this, we quantified the bias incurred for ignoring slope altogether by conducting a field study in two separate forest types: mixed conifer and mixed deciduous. The coniferous plots showed no slope-related bias whereas the deciduous plots displayed bias on steeper slopes. This difference in bias between forest types is likely due to the difficulty identifying deciduous tree tops in the digital photographs. The lack of discernible bias on the lesser slopes and in the conifer forests was largely due to the slope-related bias being overwhelmed by the unavoidable variability inherent in VPSC. Overall, the slope-related bias should be negligible, regardless of forest type, provided the majority of the sample points fall on slopes of approximately 35° or less. These results further support the use of VPSC as a useful new method of monitoring forest conditions, conducting forest inventories, or assessing wildlife habitat.

1. Introduction

Vertical point sampling (VPS) is a method by which trees are sampled with probability proportional to their squared-height (Hirata, 1955; Grosenbaugh, 1958). This method is analogous to horizontal point sampling (i.e., prism cruising in forestry) where trees are sampled with probability proportional to their squared diameter (Bitterlich, 1948; Grosenbaugh, 1958). In contrast to the wide-spread use of horizontal point sampling, VPS has rarely been used in practice, primarily due to the difficulty in implementing this procedure and to the perceived lack of usefulness of the resulting estimate of "height-squared per unit area." Recently, Ducey and Kershaw (2011) developed a method by which VPS can be quickly conducted using a digital camera. This new method alleviates many of the difficulties that arise when carrying out VPS using traditional methods. Additionally, Ducey and Kershaw (2011) show that the resulting estimates of height-squared correlate strongly with various stand-level attributes that are often time-intensive and difficult to obtain, including biomass, cubic volume, and Reineke's stand-density index (Reineke, 1933). The relationship between height-squared and these additional forest attributes makes VPS useful in ratio estimation or double-sampling schemes (Oderwald and Jones, 1992; Schreuder et al., 1993; Husch et al., 2003).

Digital cameras are increasingly popular tools for measuring different aspects of forests, trees, and crops (Clark et al., 2000; Mesas-Carrascosa et al., 2012; Murakami et al., 2012). Incorporating digital cameras into vertical point sampling greatly increases the speed, efficacy, and applicability of this method. The ubiquity and low cost of digital cameras makes vertical point sampling with a camera (VPSC) a useful tool for foresters, forest ecologists, or private land owners to rapidly assess forest conditions over a broad spatial extent or estimate aspects of forest structure that are otherwise resource intensive to obtain.

A remaining issue when conducting vertical point sampling with a camera is the effect of sloping terrain on the resulting

* Corresponding author. Present address: Yale University, School of Forestry & Environmental Studies, 195 Prospect St., New Haven, CT 06511, USA. Tel.: +1 (508) 463 5939.

E-mail addresses: daniel.maynard@yale.edu (D.S. Maynard), mjducey@unh.edu (M.J. Ducey), russ.congalton@unh.edu (R.G. Congalton), kershaw@unb.ca (J. Kershaw), joel.hartter@colorado.edu (J. Hartter).

[1] Present address: University of Colorado, Environmental Studies Program, Arts & Sciences Office Building 1, 1201 17th Street, Boulder, CO 80309, USA

0168-1699/$ - see front matter © 2013 Elsevier B.V. All rights reserved.
http://dx.doi.org/10.1016/j.compag.2013.11.007

estimates. In VPSC, a vertical photo of the canopy is taken at a randomly selected sample point and the number of tree tops appearing in the photo is tallied. On sloping terrain, the trees located uphill from the sample point appear "taller" in the resulting image, while downhill trees appear "shorter." This distortion leads to an expanded inclusion area for trees on sloping terrain that increases the probability that these trees are sampled.

In this study, we investigate two methods of accounting for sloping terrain when conducting VPSC. First, we present a method by which a novel, automated computer program is used to directly adjust for the slope at each sample point and maintain unbiased estimates. Secondly, we investigate the bias incurred for ignoring slope by conducting a field study in two separate forest types: mixed conifer and mixed deciduous. From these results we provide general recommendations as to when the slope-adjustment procedure should be followed, and when sloping terrain can be ignored with minimal bias.

2. Overview of vertical point sampling

In vertical point sampling, the radius of the inclusion area of each tree is selected to be a fixed proportion of its height, rather than a fixed proportion of its diameter (Hirata, 1955). This situation results in the inclusion area of each tree being proportional to the height squared of the tree (Grosenbaugh, 1958). A "Height Squared Factor" (HSF) is selected to control the number of trees tallied per sample point (analogous to the basal area factor, or BAF, when conducting horizontal point sampling). This HSF determines the size of the sampling area for each tree: a larger HSF means that trees have smaller inclusion areas and are sampled less often; a smaller HSF means that trees have larger inclusion areas and are sampled more often.

Ducey and Kershaw (2011) recently developed a method by which a digital camera can be used to conduct vertical point sampling. This new method allows the individual to use a photograph to identify those trees whose inclusion areas overlap a randomly selected sample point (i.e., those trees that should be tallied). Their method involves:

1. Taking a vertical photograph of the canopy at a randomly selected sample point.
2. Overlaying a rectangle on the photograph, with the dimensions of the rectangle corresponding to a pre-determined HSF.
3. Counting the number of trees tops that appear in the rectangle.
4. Multiplying this count by the corresponding HSF to obtain an estimate of height-squared per unit area.

Due to the geometry of vertical photographs, this method samples trees with probability proportional to their squared-height, and thus it is a simple way of conducting VPS. In order to simplify the geometry of this situation when dealing with sloping terrain, the method used throughout this study alters the above procedure by digitally overlaying a circle (as opposed to a rectangle) on the photograph and counting the number of tree tops located within this circle (Fig. 1). The desired HSF dictates the diameter of the overlaid circle, with a larger HSF corresponding to a smaller circle and *vice-versa*.

To understand how this photo-counting methods succeeds in implementing VPS, note that the vertical projection of a rectangular photograph can be visualized as a 4-sided inverted pyramid. By drawing a circle on the resulting image, we are projecting a cone up through the image. If the top of a tree is visible within the superimposed circle, then this is an indicator that the sample point falls within the circular inclusion area of that tree, and the tree should be tallied. Under this method, the outside boundary of a given tree's inclusion area is the collection of points where the top of a tree is at the outer edge of the cone (Fig. 2). For all such points, the distance from the camera to the tree is equal to $h \cdot \tan\theta$, where θ is half of the opening angle of the cone and h is the height of the tree. Thus, the inclusion area is a circle with radius proportional to the height of the tree, and with area proportional to the squared-height.

An important assumption with all vertical point sampling methods is that each tree has a single well-defined top that can be readily identified. In certain stands and for certain tree species this assumption is justified, though in practice it can often be difficult to identify the exact location of the "top" of the tree due to the presence of foliage or to decurrent growth forms (Fig. 1). The benefit of VPSC compared to other VPS methods is that the photos can be scored by multiple individuals and stored for later verification, thus potentially reducing the bias incurred by inaccurate estimation from any one individual. Importantly, any bias incurred by misidentifying tree tops is irrelevant in ratio or regression sampling as long as the individual is consistent in their counting preferences across all of the photographs.

2.1. A modified HSF for a circular inclusion area

Overlaying a circle on the photos alters the calculation of HSF from what Ducey and Kershaw (2011) give for a rectangular inclusion area. When overlaying a circle, the inclusion area for a tree on flat terrain is likewise a circle, equal in area to the cross-section of the cone at the point where the top of the tree intersects the cone (Fig. 2). By rewriting the radius, r, of this inclusion area in terms of the height, h, of the tree and the angle, θ, that defines the cone, the inclusion area on flat terrain is:

$$A_{flat} = \pi(h\tan\theta)^2. \quad (1)$$

If a single sample point is selected in a sampling region of area $\widetilde{A}$, the probability that this tree is included (counted) is equal to this above inclusion area divided by the total area. To estimate the total height-squared per unit area (τ), we can use a Horvitz–Thompson estimator (Horvitz and Thompson, 1952), where the summation is over the v trees counted in the photo at that point:

Fig. 1. Identifying tree tops in vertical photographs. Circles, rather than rectangles, are superimposed over the vertical photos in the modified VPSC protocol. Deciduous (left) and coniferous (right) stands each provide unique challenges to identifying tree tops.

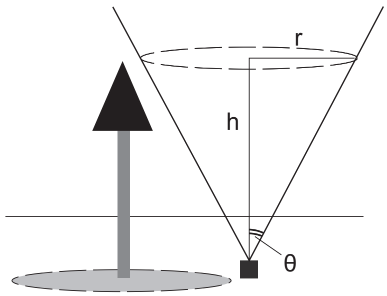

Fig. 2. The inclusion area for a tree on flat terrain. On flat terrain, the inclusion are for a tree of height h (indicated by the shaded circle) is equal to the set of points through which the top of the tree passes through the cone projected upwards by the camera. The radius of this inclusion circle can be defined in terms of the height of the tree and the angle θ, equal to half the opening angle of the cone.

$$\tau = \sum_i^v \frac{h_i^2}{\pi (h_i \tan\theta)^2/\widetilde{A}} = \frac{\widetilde{A}}{\pi \tan^2\theta} \cdot v. \tag{2}$$

Thus, we have that the HSF depends only upon the angle that defines the cone and on the total sampling area. For practical purposes, it is usually easiest to divide by the total area in order to obtain the estimate in terms of unit area per unit area. This results in a circular Height Squared Factor of:

$$HSF = \frac{1}{\pi \tan^2\theta}. \tag{3}$$

Ducey and Kershaw (2011) show that the minimum HSF of a rectangular inclusion area for a given camera can be easily reconstructed by placing the camera some known distance, K, from a wall, attaching a tape measure to the wall at the same height of the camera, and using this to measure the length, L, of the image. The width, W, of the image is then equal to this length divided by the aspect ratio of the image (assuming that the aspect ratio is written in terms of L/W). A similar process can be used to obtain the minimum HSF for a given camera when using a circular inclusion zone. First, follow the above prescription given by Ducey and Kershaw (2011) to obtain estimates of W and K. If a circle is drawn on the photo such that the diameter equals the full width of the image, then the minimum possible HSF for that camera is:

$$HSF_{min} = \frac{4 \cdot K^2}{\pi W^2}. \tag{4}$$

If a larger HSF is required (i.e., a smaller circle overlaid on the photograph), we can calculate the diameter of the new circle to be superimposed on the image by:

$$\text{New Circle Diam.} = \sqrt{\frac{HSF_{min}}{HSF_{new}}} \times (\text{Original Circle Diam.}) \tag{5}$$

For example, suppose the original image width is 20 cm with a corresponding minimum HSF of 1. If a HSF of 4 is desired, then it follows that a new circle diameter of $\sqrt{1/4} \cdot 20 = 10$ cm will yield the desired HSF.

3. The Effect of slope on VPSC

When a tree is on a slope, the point at which the top of the tree passes through the camera-cone remains parallel to the slope and is tilted from the horizontal (Fig. 3). The total area along the slope that the tree is visible within the cone is therefore equal to the intersection of a tilted plane and a cone. This results in an ellipse that is stretched both vertically along the slope and horizontally along the contour. Since sample points are generally selected using a flat projection of the study area, the inclusion area for any given tree is the projection of this sloped ellipse onto the 2-dimensional surface. This stretched and projected ellipse results in a biased sampling areas for trees located on slopes, with the severity of the bias directly related to the severity of the slope.

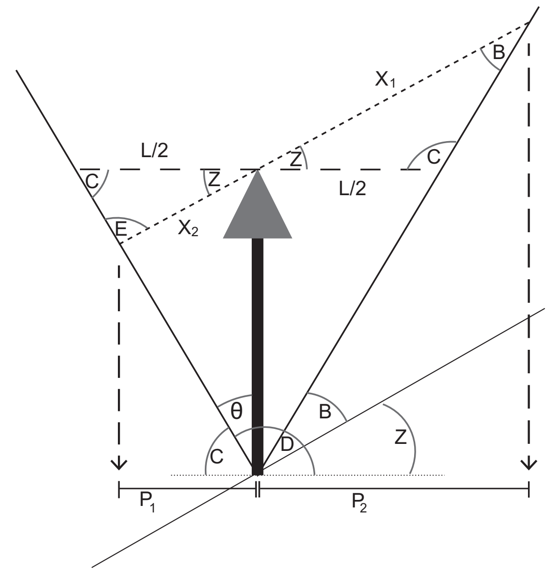

Fig. 3. The geometry of the sloped and projected inclusion area for a slope of A degrees. The wide dashed line and the small dashed line show where the tree top passes through the cone on flat terrain and sloping terrain, respectively. The sum of the lengths P_1 and P_2 gives the length of the major radius of the projected elliptical inclusion area, which can be written in terms of the angles θ, B, C, D, E, and the original inclusion radius, L.

Grosenbaugh (1958) and Hirata (1955) recognized this slope-bias and provided a series of detailed adjustments to correctly account for slope on a tree-by-tree basis. Since VPSC is not conducted on a tree-by-tree basis, these correction methods are are not feasible. Here, we address these limitations by deriving the ratio of the sloped inclusion area to the flat inclusion area for a tree of fixed height. We then present a simple method by which this ratio is used to correctly adjust for slope at the plot level (rather than on a tree-by-tree basis) in order to maintain unbiased estimates in VPSC.

Consider a tree of height h on a slope of Z degrees (Fig. 3). Suppose a HSF is used such that θ is half of the opening angle of the cone (see Eq. (3)), and the radius of the inclusion area is given by L. Let $C = 90 - \theta$, $B = C - Z$, $D = 180 - C$, and $E = 180 - C - Z$. Let X_1 and X_2 be the two segments that define the length of the sloped inclusion area. It follows that the interior angles of the two triangles bounded by the cone, the original inclusion radius, and the new inclusion length can be written in terms of Z, B, C, D, and E (Fig. 3). Using the law of sines, we have that:

$$\frac{\sin E}{L/2} = \frac{\sin C}{X_1} \Rightarrow X_1 = \frac{\sin C}{\sin E} \cdot \frac{L}{2}, \tag{6}$$

and

$$\frac{\sin B}{L/2} = \frac{\sin D}{X_2} \Rightarrow X_2 = \frac{\sin D}{\sin B} \cdot \frac{L}{2}. \tag{7}$$

Let P_1 and P_2 be the segments that correspond to the horizontal projections of X_1 and X_2, respectively. Then from Eqs. (6) and (7) it follows that:

$$P_1 = X_1 \cdot \cos Z = \frac{\sin C}{\sin E} \cdot \frac{L}{2} \cdot \cos Z = S_1 \cdot \frac{L}{2}, \tag{8}$$

and

$$P2 = X_2 \cdot \cos Z = \frac{\sin D}{\sin B} \cdot \frac{L}{2} \cdot \cos Z = S_2 \cdot \frac{L}{2}, \tag{9}$$

where

$$S_1 = \frac{\sin C}{\sin E} \cdot \cos Z \tag{10}$$

$$S_2 = \frac{\sin D}{\sin B} \cdot \cos Z. \tag{11}$$

As the intersection of a cone and a plane forms an ellipse, and the projection of an ellipse onto a single axis remains an ellipse, we have that the 2-dimensional projected inclusion area is likewise an ellipse (Grosenbaugh, 1958), with the length along the major axis being $P_1 + P_2$. Note that P_1 corresponds to the distance from the tree to the projected lower edge of the inclusion zone, and P_2 corresponds to the distance from the tree to the projected upper edge of the inclusion zone. If we change coordinates so that the center of the projected inclusion area is at the center of the X–Y coordinate plane, then it follows that the tree is projected down to the point $(x, y) = (-(P_2 - P_1)/2, 0)$ (Fig. 4).

Also note that the the original inclusion circle had a diameter of L. The sloped inclusion area can be viewed as the intersection of the cone and of a plane that has been horizontally rotated about the base of the tree. Thus, the width of the sloped inclusion area (along the contour) at the the base of the tree remains L.

Combining these two results, we know that at the outer edge of the inclusion area must pass through the point (Fig. 4):

$$(x, y) = \left(\frac{-(P_2 - P_1)}{2}, \frac{L}{2}\right) = \left(\frac{-(S_2 - S_1)}{2} \cdot \frac{L}{2}, \frac{L}{2}\right). \tag{12}$$

Noting that the major radius, a, of the projected ellipse is equal to $(S_1 + S_2)/2 \cdot L/2$, we can substitute the above point into the equation of an ellipse, and solve for the minor radius, b:

$$1 = \frac{x^2}{a^2} + \frac{y^2}{b^2} \Rightarrow 1 = \frac{\left(\frac{S_2 - S_1}{2}\right)^2 \left(\frac{L}{2}\right)^2}{\left(\frac{S_1 + S_2}{2}\right)^2 \cdot \left(\frac{L}{2}\right)^2} + \frac{\left(\frac{L}{2}\right)^2}{b^2} \Rightarrow b = \frac{L}{2} \cdot \left(\frac{S_1 + S_2}{2\sqrt{S_1 \cdot S_2}}\right). \tag{13}$$

From this, we can calculate the projected elliptical inclusion area for this tree:

$$A_{slope} = \pi ab = \pi \left[\frac{L}{2} \cdot \left(\frac{S_1 + S_2}{2}\right)\right] \left[\frac{L}{2} \cdot \left(\frac{S_1 + S_2}{2\sqrt{S_1 \cdot S_2}}\right)\right] = \pi \left(\frac{L}{2}\right)^2 \cdot \frac{(S_1 + S_2)^2}{4\sqrt{S_1 \cdot S_2}}. \tag{14}$$

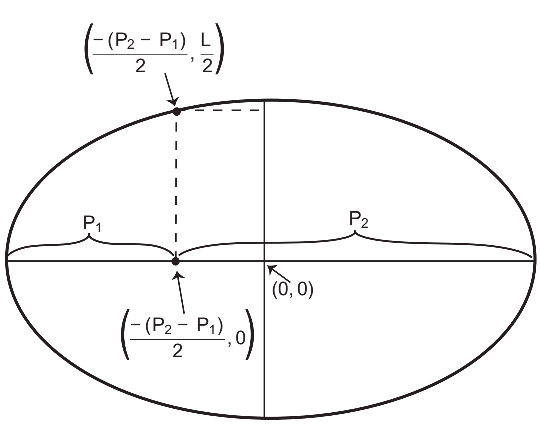

Fig. 4. Top-down view of the projected inclusion area with major radius equal to $P_1 + P_2$. The tree is projected downward to the point $(-(P_2 - P_1)/2, 0)$, and the width of the ellipse at this point is equal to the original radius of the circle, L.

Since the inclusion area along flat terrain is $A_{flat} = \pi(L/2)^2$, we have that the slope adjustment factor, α, is:

$$\alpha = \frac{A_{slope}}{A_{flat}} = \frac{(S_1 + S_2)^2}{4\sqrt{S_1 \cdot S_2}} = \frac{\left(\tilde{S_1} + \tilde{S_2}\right)^2}{4\sqrt{\tilde{S_1} \cdot \tilde{S_2}}} \cdot \cos Z, \tag{15}$$

where

$$\tilde{S_1} = \frac{\sin C}{\sin E} \quad \text{and} \quad \tilde{S_2} = \frac{\sin D}{\sin B}. \tag{16}$$

An important property of this adjustment factor is that it does not depend on the height of the tree, h, or on the height-dependent inclusion radius, L. Therefore, every tree located on the same uniform slope has an inclusion area that is expanded by the same factor.

The behavior of the adjustment percentage (the adjustment factor, α, expressed as a percent) is displayed in Table 1 for various HSFs and slopes. In this table, the "Field of View" corresponds to the angular field of view of the cone, i.e., 2θ. We see that for relatively moderate HSFs above 3, the increase in the inclusion area on sloping terrain is less than 10% until slopes of 30–40° are reached. For lower HSFs, slopes of 20° or less likewise result in an increase in the inclusion area of approximately 10% or less.

3.1. Adjusting for slope

There will likely be some instances where a low HSF is required (such as in very open stands) or where a large proportion of sample points fall on steep terrain. In these settings, it will be beneficial to adjust for slope so that trees on steeper slopes are not over-sampled. To adjust for this expanded inclusion area we employed a novel variable-radius circle technique, where the size of the superimposed circle depends on the severity of the slope. In this setting, photos taken on steeper slopes will have a smaller circle superimposed on them, so that, for any given tree, the stretched and projected inclusion area corresponding to this smaller circle is equal in area to its original circular inclusion area on flat terrain. While the shapes of these inclusion areas will be different, all that is required to maintain design unbiased estimates is that their inclusion areas are identical.

More specifically, if θ is the angle that corresponds to the desired HSF on flat terrain, we need to select a smaller angle, θ', such that the projected inclusion area on sloping terrain defined by this narrower angle is equal to the original circular inclusion area on flat terrain. For a given tree of height h, that entails solving the following equality for θ' (the use of the prime denotes a variable related to the narrower cone and smaller superimposed circle):

$$A'_{slope} = A_{flat} \Rightarrow \alpha' \pi h^2 \tan^2 \theta' = \pi h^2 \tan^2 \theta \Rightarrow \alpha' \cdot \tan^2(\theta') - \tan^2(\theta) = 0. \tag{17}$$

Table 1
The inclusion area adjustment factor (expressed as a percent), for various height squared factors and slopes.

HSF	1	2	3	4	5	6	7
Field of view[a]	59	43	36	32	28	26	24
Slope (°)							
0	0	0	0	0	0	0	0
10	2	1	0	0	0	0	0
20	7	3	2	2	1	1	1
30	18	9	6	4	3	3	2
40	46	20	12	9	7	6	5
50	146	47	28	20	15	12	11

[a] Refers to the angular field of view (i.e. 2θ) of the cone in degrees.

Since α' in Eq. (17) is also a function of θ', this equation cannot be solved in closed form. It can, however, be numerically solved without difficulty in most statistical or mathematical software packages (see Supplemental material).

Given the above results, the variable-radius circle procedure for correctly adjusting for slope when conducting VPSC is:

1. Select a desired HSF and calculate the corresponding circle diameter using Eqs. (4) and (5).
2. For those sample points on flat terrain, superimpose a circle of this diameter on the images and count the tree tops in each photo.
3. For each sample point on sloping terrain, solve Eq. (17) for the new angle θ', and calculate the new HSF and corresponding image circle radius using Eqs. (3) and (5).
4. Superimpose this smaller circle on the vertical photograph, and count the number of tree tops in this smaller superimposed circle. Do this for each image taken on sloping terrain.
5. Add the total number of trees counted across all photographs, multiply by the HSF, and divide by the number of sample points to obtain an estimate of height-squared per unit area.

For two trees of the same height, one on flat terrain and one on a slope, this procedure results in the same inclusion area for both. Therefore it maintains the requirements of sampling with probability proportional to height-squared, and will result in design-unbiased estimates.

4. Field study: bias assessment

The variable-radius procedure outlined above might limit the usefulness of VPS with a camera, as it involves access to and knowledge of statistical or mathematical computer software. We therefore conducted a two-part field study to quantify the bias incurred for ignoring slope altogether. The goals of this field study were fourfold: (1) quantify the bias in the photo counts for different values of the slope adjustment factor; (2) identify a slope adjustment factor threshold, below which bias will be negligible in real-world settings; (3) investigate how forest type (deciduous vs. coniferous) affects this slope-related bias; and (4) compare how different sources of variability impact this bias.

4.1. Study design

The study took place in two separate regions: Pawtuckaway State Park in Nottingham, New Hampshire during November of 2010 (after leaf fall), and in the counties of Union and Baker in northeast Oregon during the summers of 2011 and 2012. Pawtuckaway State park is located in southeastern New Hampshire is primarily comprised of deciduous mixed-oak forests dominated by red oak (*Quercus rubra*), American beech (*Fagus grandifolia*), sugar maple (*Acer saccharum*), eastern white pine (*Pinus strobus*), and eastern hemlock (*Tsuga canadensis*). Conversely, the forests in Baker and Union counties are populated almost exclusively by dry upland forest communities comprised primarily of ponderosa pine (*Pinus ponderosa*), grand fir (*Abies grandis*), Douglas fir (*Pseudotsuga menziesii*), and western larch (*Larix occidentalis*).

We selected thirty-three sample points in the deciduous forest and thirty-four sample points in the coniferous forest. These points were opportunistically chosen in order to obtain a near-uniform distribution of slopes. Once a general location was selected, the exact sample point location was randomized to an area within a 20-m radius circle. At each sample point, we took a vertical photograph, measured the slope, and conducted a prism sweep using a metric BAF of 4.6 m^2/ha (20 ft^2/ac) for the deciduous plots, and a metric BAF of 4 m^2/ha (17.4 ft^2/ac) for the coniferous plots. The camera was held by hand 1 m above the ground and was equipped with a bubble level to ensure that it was held vertically. We measured diameter at breast height (DBH) for each tree tallied using the prism sweep. For the deciduous plots, we determined the height of every fourth tree with a clinometer and laser rangefinder. For the coniferous plots, we used a metric BAF of either 9 m^2/ha (39.2 ft^2/ac), or 16 m^2/ha (69.7 ft^2/ac) to identify trees for height measurement. The specific choice of BAF was selected in order to obtain approximately 2–4 height trees per plot, and was based on an visual assessment of stand density.

The resulting digital photographs were scored by ten separate participants for each forest type. These participants were all graduate students or professors with backgrounds in the natural resources, forestry, biology, wildlife ecology, or geography. Each individual was shown the same image twice: once with the image overlaid with the unadjusted circle corresponding to the nominal HSF, and once with the image overlaid with a variable-radius circle (using the above slope adjustment) that correctly adjusted for the slope at that sample point. The individuals were given no training or practice beforehand; they were instructed simply to count the number of tree tops within each circle on each photograph, and to subjectively differentiate between tree branches and tree tops to the best of their ability. The photos were displayed in a random order to each participant so as to avoid any trend-bias in the counting process. For the deciduous forest, this process resulted in 66 photos scored by each participant, and 660 photos scored in total. For the coniferous forest, this process resulted in 68 photos scores by each participant, and 680 photos scored in total.

The overlaying of the circles on the photos and the numerical analysis for Eq. (17) was carried out in Matlab (MathWorks Inc., 2010). The width of the lines of these overlaid circles was set equal to one pixel to minimize the number of border-line trees (i.e., those tree tops that fell exactly on the line and could not be visually distinguished between being "in" or "out"). The digital photos were displayed in color, with on-screen dimensions of approximately $6.5\ \text{cm} \times 10\ \text{cm}$ (about $2.5\ \text{in} \times 4\ \text{in}$). The participants were not able to zoom in or move the image on the screen, and they were prompted to enter the number of trees in a text box on the screen. The Matlab programs and supporting documentation for analyzing these data are available as Supplemental material.

For the deciduous forest, we used a HSF of 1 to allow for adequate assessment of the relative impact of different adjustment percentages. We used a comparable HSF of 1.4 for the coniferous forest (due to differing camera characteristics a HSF of 1 was not feasible). Table 1 shows that the adjustment percentages for a HSF close to 1 attain a relatively uniform distribution of values from 2% to 46% as the slope increases from ten to forty degrees, whereas HSFs larger than 1 have a more limited range of adjustment percentages. Furthermore, a HSF significantly larger than 1 should almost always be used in practice (Ducey and Kershaw, 2011), so these results also serve as a conservative estimate of the upper limit of the effect of slope.

4.2. Statistical analysis

The approach taken here to analyze the effect of various sources of variability in the photo counts is motivated by the analytical methods employed by Ringvall and Stahl (1999). Here, a mixed-effects model was utilized to investigate the overall effect of slope on the count in each photo. The outcome of interest was the count on the *i*th photo by the *k*th participant on the *j*th plot. The specific model was:

$$\Psi(Count_{ijk}) = \beta_0 + \beta_1 \cdot \overline{\text{tree height}_j} + \beta_2 \cdot I_i(0,10) + \beta_3 \cdot I_i(10,20) + \beta_4 \cdot I_i(20,30) + \beta_5 \cdot I_i(30,\infty) + \beta_8 \cdot \text{plot}_j + \beta_9 \cdot \text{person}_k + \beta_{10} \cdot \text{plot}_j \times \text{person}_k + \epsilon_{ijk}, \quad (18)$$

where $\overline{\text{tree height}_j}$ is the average tree height for the jth plot (calculated using a ratio estimator along with DBH); and where $I_s(X,Y) = 1$ when $X < slope_i \leqslant Y$ for the unadjusted photos, and equals zero otherwise. For the adjusted photos, all indicator variables were set equal to zero. In this model, each of the factors $\exp(\beta_2), \ldots, \exp(\beta_5)$ corresponds to the relative increase in the photo count incurred for failing to account for slopes of 0–10°, 10–20°, 20–30°, and >30°, respectively.

This model was fit separately for the deciduous and coniferous data. In both models, slope and average tree height per plot were included as fixed effects. Plot, person, and the interaction of person × plot were included as random effects. The variable corresponding to average tree height was normalized to give a mean of zero and standard deviation of one. The reported coefficients for average tree height therefore correspond to an increase of one standard deviation from the mean. Since the count data were roughly poisson distributed, $\Psi(\cdot)$ was modeled using the quasi-Poisson log-link function. The quasi-Poisson model differs from a Poisson model only in that it does not assume the variance exactly equals the mean, and so it allows for greater flexibility in the model-fitting process (i.e., it allows for overdispersion). Approximate p-values and 95% confidence intervals are reported for each covariate, though it should be noted that these statistics are not exact for mixed-effects models.

A mixed-effects analysis of variance (ANOVA) model was fit to the data in order to compare the relative contribution of each factor to the overall variability in the log of the photo counts. Average tree height, slope, person, and plot were included as main sources of variation, and the random effects of plot, person, and plot × person were modeled via the error term. As the counts were Poisson distributed, the square root of the counts were approximately normally distributed. To test the appropriateness of this assumption, residual plots and Q–Q plots were examined, indicating no violations of independent, normally distributed, and heteroscedastic errors. For the ANOVA model, tests of significance were conducted using F-tests and corresponding p-values are reported.

Estimates of height-squared per unit area were calculated for each person for both the unadjusted and slope-adjusted photos, and a paired Student's t-test was used to compare the difference in these estimates. Pearson's correlation coefficient was used for all reported correlations. All statistical analyses were carried out in R (R Core Team, 2012), with the mixed effects model and ANOVA model being implemented via *glmer* and *aov* functions in the "lme4" and "stats" packages, respectively.

4.3. Results

Across the 33 deciduous plots, we identified a total of 216 trees using the prism sweep and we obtained a height measurement for 54 of these trees. Across the 34 coniferous plots, we identified a total of 190 trees using the prism sweep, and we obtained a height measurement for 104 of these. The forest types were roughly comparable in quadratic mean diameter (QMD), height, and basal area, with the deciduous plots being almost twice as dense as the coniferous plots (Table 2).

Table 2
Stand-level attributes for the 33 deciduous plots and 34 coniferous plots.

Attribute	Mean	S.D.	Range
Mixed-deciduous forest (n = 33)			
Quadratic mean diameter (cm)	31	11	(11,51)
Height[a] (m)	20.2	8.2	(10.0,46.8)
Basal area (m^2/ha)	30.1	9.9	(18.4,55.1)
Trees per hectare	658.5	762.0	(120,3767)
Coniferous forest (n = 34)			
Quadratic mean diameter (cm)	36	13	(10,67)
Height[a] (m)	22.9	7.0	(7.3,36.1)
Basal area (m^2/ha)	28.5	19.9	(4.0,90.0)
Trees per hectare	394.5	431.0	(20.3,2142.5)

[a] Calculated using ratio estimators along with DBH.

The distribution of slopes was likewise comparable between the two forest types. Out of the 33 sample deciduous points, the average slope was 21.4°, with 6 sample points taken on slopes less than 10°, 9 taken on slopes between 10° and 20° (including 20°), 12 taken on sloped between 20° and 30° (including 30°), and 6 taken on slopes greater than 30°. For the 34 coniferous sample points, the average slope was 21.3, with 6 sample points taken on slopes less than 10°, 9 taken on slopes between 10° and 20° (including 20°), 11 taken on sloped between 20° and 30° (including 30°), and 8 taken on slopes greater than 30°.

The correlation between different individuals' photo counts was significantly higher with the coniferous plots than the deciduous plots. The mean inter-subject correlation was 0.92 ± 0.03 for the coniferous plots, and 0.70 ± 0.14 for the deciduous plots. This difference likely reflects the decurrent growth forms of deciduous trees and the subjectivity inherent in identifying deciduous tree tops versus tree branches. For the deciduous plots, the overall mean was 6.8 ± 0.5 trees counted in the adjusted photos and 7.4 ± 0.5 trees counted in the unadjusted photos ($p < 0.001$ for t-test of difference in means); for the coniferous plots, the overall mean was 5.7 ± 0.2 trees counted in the adjusted photos and 5.8 ± 0.2 trees counted in the unadjusted photos ($p = 0.13$ for t-test of difference in means).

For the deciduous mixed-effects regression model, a statistically significant effect of failing to adjust for slope was only observed on those plots occurring on >30° slope (Table 3). These plots also yielded the largest increase in the count, with a relative increase of 18% (95% CI = [1.02, 1.36], $p = 0.02$). For plots on 0–10°, 10–12°, and 20–30° slopes, failing to adjust for slope resulted in an increase in the count by less than 10%, with reduction factors of 1.06, 1.05, and 1.09, respectively; none of these values showed a statistically significant deviation from the null value of 1. In the coniferous mixed-effects regression model there was no discernible impact of slope across any of the slope categories (Table 3). The relative change in count ranged from a 3% reduction on 0–10° slopes, to a 5% increase on 10–20° and >30° slopes. None of these slope effects exhibited any degree of statistical significant ($p \gg 0.05$ in all cases).

After controlling for slope, individual, and average tree height, the overall effect of slope was minimal in the mixed-effects ANOVA model (Table 4). Differences in slope accounted for only 1.2% and 0.1% of the overall variability in photo counts for the deciduous and coniferous plots, respectively. This effect was statistically significant for the deciduous plots ($p < 0.001$), but not significant for the coniferous plots ($p = 0.18$). Average tree height accounted for 19.2% of the variability in count among the coniferous plots, but only 7.6% of the variability in count among the deciduous plots ($p < 0.001$ in both cases). In both forest types, the random differences between plot accounted for 44.3% and 65.9% of the variation in the for deciduous and coniferous plots, respectively. Individual counting preferences were markedly more pronounced among the deciduous plots, contributing 22.9% of overall variability for the deciduous plots, and only 4.9% of the variability for the coniferous plots.

Table 3
Results from the mixed-effects regression models (only fixed effects are reported).

Fixed effect	Factor[a]	95% C.I.	p-Value
Deciduous forest plots			
Intercept[b]	6.33	(5.32, 7.54)	<0.001
Avg. tree height[c]	1.14	(1.02, 1.27)	0.02
Slope (°)			
0–10	1.06	(0.93, 1.20)	0.37
10–20	1.05	(0.94, 1.17)	0.37
20–30	1.09	(0.99, 1.20)	0.07
>30	1.18	(1.02, 1.36)	0.02
Coniferous forest plots			
Intercept[b]	4.66	(3.74, 5.79)	<0.001
Avg. tree height[c]	1.45	(1.18, 1.78)	<0.001
Slope (°)			
0–10	0.97	(0.80, 1.17)	0.74
10–20	1.05	(0.92, 1.19)	0.49
20–30	0.98	(0.88, 1.10)	0.73
>30	1.05	(0.94, 1.18)	0.40

[a] Equal to exp(coefficient).
[b] Equivalent to the estimated average tree count for the slope-adjusted photo.
[c] Corresponds to an increase of one standard deviation from the mean.

Table 4
Results from the mixed-effects ANOVA models.

Source	D.f.	Sum of squares	% Variance[b]	p-Value[a]
Deciduous forest plots				
Avg. tree height	1	17.5	7.6	<0.001
Plot	30	101.7	44.3	<0.001
Individual	8	52.6	22.9	<0.001
Slope class	4	2.8	1.2	<0.001
Plot × Individual	287	34.5	15.0	<0.001
Error	326	20.8	9.0	
Coniferous forest plots				
Avg. tree height	1	81.2	19.2	<0.001
Plot	31	278.7	65.9	<0.001
Individual	8	20.63	4.9	<0.001
Slope class	4	0.2	0.1	0.18
Plot × Individual	296	32.3	7.6	<0.001
Error	336	10.2	2.4	

[a] Testing the null hypothesis H_0: no difference between source components.
[b] Calculated as the percentage of the total sum of squares for each source factor.

4.4. Discussion

Two methods of accounting for sloping terrain were investigated in this study: (1) maintaining unbiased estimates by superimposing variable-radius circles to adjust for the slope at each sample point and (2) ignoring slope altogether, provided that the HSF is appropriately selected and the majority of sample points are located on moderately sloping terrain (approximately 35° or less). The decision about which of these two options to use will depend heavily on the intended use of the information. The variable-radius circle technique presented in this study is a simple and intuitive way to adjust for slope to maintain unbiased estimates, regardless of the selected HSF or of the severity of the sloping terrain. If one aims to correlate the individual sample point estimates of height-squared to other measurements taken at that sample point, (e.g., in a double-sampling scheme to estimate board foot volume for a timber harvest), then directly adjusting for slope would likely be beneficial. Conversely, if an individual or a group is simply interested in quickly assessing different elements of vertical structure in order to make qualitative inferences about stand structure then there will be minimal need or desire to directly adjust for slope.

As discussed, this study used a HSF of approximately 1 in order to quantify the slope-related bias across a wide range of slope adjustment percentages. This HSF of 1 corresponds to adjustment percentages ranging from 2% on 10° slopes to 46% on 40° slopes. To interpolate these results to those situations that employ a HSF other than 1, we can compare similar slope adjustment percentages between the new HSF and the reference HSF of 1. For example, with a HSF of 4 the slope adjustment percentage is about 2% on 20° slopes (Table 1). With a HSF of 1, a 2% slope adjustment percentage occurs on slopes of 10°. Therefore, the expected bias incurred on 20° slopes with a HSF of 4 is equivalent to the bias incurred on 10° slopes with a HSF of 1.

Our results show that much of the slope-related bias is effectively overwhelmed by a combination of the inherent variability in individuals' counting preferences, by plot differences (foliage, tree species, etc.), and by differences in tree heights. Approximately 99% of the observed variability between photo counts was due to these factors, while roughly 1% of the variability in the photo counts was due to slope bias. The only significant effect of slope in this study was observed on >30° slopes in the deciduous plots, which corresponds to slope adjustment percentages of 19–46%. Ducey and Kershaw (2011) recommend a HSF between 3 and 6, where comparable adjustment percentages of 19–46% are not encountered until slopes of >40° are reached. Accordingly, an appropriately selected HSF will result in negligible or non-existent bias in most real-world settings where the large majority of sample points fall on slopes less than 40°. To be conservative, 35° is a reasonable cut-point in practice, below which slope-bias should be negligible.

In very dense stands (or in sparser stands with very tall trees) the density of tree tops in the image will be relatively high. In such settings, even small changes in the size of the superimposed circles can exclude many trees from being counted. While this would seem to imply that slope bias will be greater in dense stands, the selection of an appropriately large HSF can minimize this bias. A HSF between 3 and 6 will generally provide a "good" number of sample trees (roughly 6–9 trees) tallied per photo (Ducey and Kershaw, 2011). In denser stands, a HSF of 6 or higher may be needed to ensure that only 6–9 trees appear in the unadujsted photos. Accordingly, an appropriately selected HSF will minimize slope bias in two ways: (1) it will reduce the impact of slope via reduction in the corresponding slope adjustment percentages and (2) it will minimize the impact of stand density by reducing the number of trees that appear within the circle, and therefore reduce the probability that a tree will be excluded due to a smaller superimposed circle.

In this study, the HSF was much smaller than should be selected in practice, yet the impact of slope was non-existent in the coniferous stands and negligible on slopes less than 30° in the deciduous stands. For deciduous trees, distinguishing between tree branches and tree tops is generally much more difficult than for coniferous trees (see Fig. 1). Accordingly, small changes in circle radii likely resulted in both branches and tree tops being excluded. In this experiment, adjusting the circles for slope generally reduced the overlaid circle radii by less than 10%. For an on-screen photograph measuring approximately 6.5 cm × 10 cm (approximately 2.5 in × 4 in) this translated into a reduction in the radius of the overlaid circle by less than 5 mm in all instances, and in most cases only by 2 or 3 mm. Only on slopes over 30°, where adjustment percentages were greater than 15–20%, did the differences in the radii of the overlaid circles approach 5 mm. This tiny reduction in the size of the overlaid circle likely explains the negligible impact of slope in the coniferous setting, but the exclusion of deciduous branches likely led to small but significant (and potentially incorrect) reductions in the count. As with dense stand, selection of an appropriately large HSF can mitigate the erroneous over-counting of branches.

This study was subject to several limitations. The slope correction method presented here assumes a smooth, uniform slope that is rarely encountered in practice. Measurements of slope at each sample point are often imprecise estimates of the average slope within the immediate vicinity on the plot. In horizontal point sampling with a prism or angle gauge, the vertical displacement of each individual tree relative to plot-center can be adjusted for in order to maintain accurate inclusion probabilities for each tree, regardless of the heterogeneity of the slope (Beers, 1969). VPSC is not conducted on a tree-by-tree basis, so there is no obvious extension of this method to account for irregular slopes. In such settings, the randomness of terrain irregularities likely leads to minimal systematic bias in the overall estimate, but more research into this problem is warranted. Lastly, boundary correction methods for those sample points that fall close to the stand edge have yet to be investigated. Grosenbaugh (1958) outlines one such technique when conducting VPS on a tree-by-tree basis using traditional techniques, but these methods likewise have no immediate extension to VPSC.

Despite these limitations, the results of the bias assessment presented here suggest an upper bound on the expected bias incurred for failing to adjust for slope, given that the HSF is selected appropriately. Perfectly accurate estimates of height-squared will probably not be needed for most applications of VPSC, and the bias that will be incurred by sloping terrain will have minimal influence. If, however, very accurate and precise estimates of height-squares are desired even on moderately sloping terrain, then the methods presented in the paper outline an intuitive way to adjust each photo to correctly account for slope using variable-radius photos. If circles are already being digitally superimposed on the images to obtain a desired HSF, then adjusting these circles to account for slope is a simple process.

4.5. Conclusions

Vertical point sampling with a camera is appealing in those settings where an individual or a group is interested in improving their estimation of forest structure without investing substantial time, money, or resources, particularly when forest structure or health needs to be rapidly assessed over a broad spatial extent. Since it requires no formal training and requires no investment in additional equipment (provided the user has access to a digital camera), VPSC should appeal to a broad array of individuals, including regional foresters, researchers, and private land owners. The results presented here indicate that vertical point sampling with a camera can be employed regardless of sloping terrain, either by directly adjusting for slope or by ignoring slope altogether.

Acknowledgement

The Communities and Forests in Oregon (CAFOR) project, with support by a grant from the Disaster Resilience for Rural Communities Program, which is part of the National Institute of Food and Agriculture program of the U.S. Department of Agriculture (Award #2010-67023-21705).

The New Hampshire Agricultural Experiment Station.

Appendix A. Supplementary material

Supplementary data associated with this article can be found, in the online version, at http://dx.doi.org/10.1016/j.compag.2013.11.007.

References

Beers, T.W., 1969. Slope correction in horizontal point sampling. J. Forest. 67 (3), 188–192.
Bitterlich, W., 1948. Die Winkelzahlprobe. Allg. Forst Holzwirtsch. Ztg. 59 (1/2), 4–5.
Clark, N., Wynne, R., Schmoldt, D., Winn, M., 2000. An assessment of the utility of a non-metric digital camera for measuring standing trees. Comput. Electron. Agric. 28 (2), 151–169.
Ducey, M.J., Kershaw, J.A., 2011. Vertical point sampling with a camera. Northern J. Appl. Forest. 28 (2), 61–65.
Grosenbaugh, L.R., 1958. Point-Sampling and Line-Sampling: Probability Theory, Geometric Implications, Synthesis. US Forest Service Miscellaneous Paper 60, US Forest Service, Southern Forest Experiment Stat.
Hirata, T., 1955. Height estimation through Bitterlich's method – vertical angle count sampling. Jpn. J. Forest. 37 (11), 479–480.
Horvitz, D.G., Thompson, D.J., 1952. A generalization of sampling without replacement from a finite universe. J. Am. Stat. Assoc. 47 (260), 663–685.
Husch, B., Beers, T.W., Kershaw, J.A., 2003. Forest Mensuration, fourth ed. John Wiley & Sons, Hoboken, NJ.
MathWorks Inc., 2010. MATLAB. Version R2010a, Natick, MA.
Mesas-Carrascosa, F.J., Castillejo-González, I.L., de la Orden, M.S., García-Ferrer, A., 2012. Real-time mobile phone application to support land policy. Comput. Electron. Agric. 85, 109–111.
Murakami, T., Yui, M., Amaha, K., 2012. Canopy height measurement by photogrammetric analysis of aerial images: application to buckwheat (Fagopyrum esculentum Moench) lodging evaluation. Comput. Electron. Agric. 89, 70–75.
Oderwald, R.G., Jones, E., 1992. Sample sizes for point, double sampling. Can. J. Forest Res. 22, 980–983.
R Core Team, 2012. R: A Language and Environment for Statistical Computing. R Foundation for Statistical Computing, Vienna, Austria. <http://www.r-project.org>.
Reineke, L.H., 1933. Perfecting a stand-density index for even-aged forests. J. Agric. Res. 46 (7), 627–638.
Ringvall, A., Stahl, G., 1999. Field aspects of line intersect sampling for assessing coarse woody debris. Forest Ecol. Manage. 119, 163–170.
Schreuder, H.T., Gregoire, T.G., Wood, G.B., 1993. Sampling Methods for Multiresource Forest Inventory. John Wiley & Sons, New York.